

# INTERNATIONAL SOCIETY FOR SOIL MECHANICS AND GEOTECHNICAL ENGINEERING



*This paper was downloaded from the Online Library of the International Society for Soil Mechanics and Geotechnical Engineering (ISSMGE). The library is available here:*

<https://www.issmge.org/publications/online-library>

*This is an open-access database that archives thousands of papers published under the Auspices of the ISSMGE and maintained by the Innovation and Development Committee of ISSMGE.*

# Prestress Induced in Consolidated-quick Triaxial Tests

## Précontrainte induite au cours d'essais de compression triaxiale rapide

by A. CASAGRANDE, Professor, Harvard University, Cambridge, and S.D. WILSON, Harvard University, Cambridge, Mass., U.S.A.

### Summary

For consolidated-quick (Qc) triaxial compression tests the effective principal stress ratio at failure was found to be higher than that in slow (S) tests. This apparent contradiction is explained by the fact that in a Qc test the specimen is really prestressed because during the entire test the effective stresses are steadily falling. The results of Qc tests on undisturbed samples of a firm inorganic clay and of a soft organic clay are presented and analysed from this viewpoint.

### Introduction

In a slow (S) triaxial compression test, the specimen is first fully consolidated under an all-around pressure exceeding the natural preconsolidation stress, and then the axial stress increased so slowly that practically no increase in pore pressure develops. Therefore, the effective stresses may be assumed equal to the externally applied stresses and the angle of internal friction ( $\varphi$ ) may be computed from the equation:

$$\frac{\sigma_1}{\sigma_3} = \tan^2 \left( 45 + \frac{\varphi}{2} \right)$$

where  $\sigma_1$  = major principal stress  
 $\sigma_3$  = minor principal stress = consolidation pressure.

When the results of a series of S tests on a fully saturated undisturbed clay are plotted in the form of Mohr stress circles, the envelope to the circles for failure stresses is found to be a straight line for normal stresses in excess of the natural preconsolidation stress. For normal stresses below the natural preconsolidation stress the envelope is found to curve above the straight line continuation to the origin, resulting in higher principal stress ratios (Fig. 1).

In a consolidated-quick (Qc) triaxial compression test, no drainage is permitted during application of the deviator stress ( $p = \sigma_1 - \sigma_3$ ) and therefore some of the load is carried by the pore water. If one measures the pore pressure ( $u$ ) by means

### Sommaire

On a trouvé que dans les essais de compression triaxiale «rapides» (essais Qc), le taux effectif de contrainte à la rupture était plus élevé que dans les essais de compression lente (essais S). Cette apparente contradiction s'explique par le fait que dans un essai Qc l'échantillon est en réalité précomprimé, parce que, pendant toute la durée de l'épreuve, les efforts effectifs diminuent constamment. Les résultats des essais Qc sur des échantillons non remaniés d'une argile ferme inorganique et d'une argile organique tendre sont présentés et analysés suivant ce point de vue.

of a suitable device, the effective stresses can be computed as follows:

$$\begin{aligned} \bar{\sigma}_3 &= \sigma_c - u \\ \bar{\sigma}_1 &= \bar{\sigma}_3 + p \end{aligned}$$

Where  $\bar{\sigma}_3$  = effective minor principal stress  
 $\bar{\sigma}_1$  = effective major principal stress  
 $\sigma_c$  = constant chamber (all-around) pressure  
 $u$  = pore pressure  
 $p = (\sigma_1 - \sigma_3)$  = deviator stress.

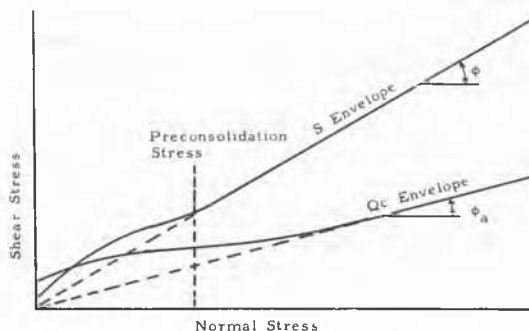


Fig. 1 Typical Failure Envelopes for Qc and S Tests  
 Courbes intrinsèques caractéristiques des essais Qc et S

Since in a Qc test the effective minor principal stress at failure is always considerably smaller than at the start of the test, it follows that the specimen is being tested in a range of prestress. Therefore, it is not surprising that the effective principal stress ratio at failure is higher than the principal stress ratio as determined by *S* tests.

### Description of Materials Tested

**Organic Clay.**—A marine deposit containing many small shells and an occasional larger shell; very soft, yet brittle in the undisturbed state, and extremely soft and sticky upon remolding. The natural water content ranges between 90 and 100%, which is somewhat above the liquid limit. The results of Atterberg limit tests, shown in Fig. 2, indicate also that this material is an organic clay.

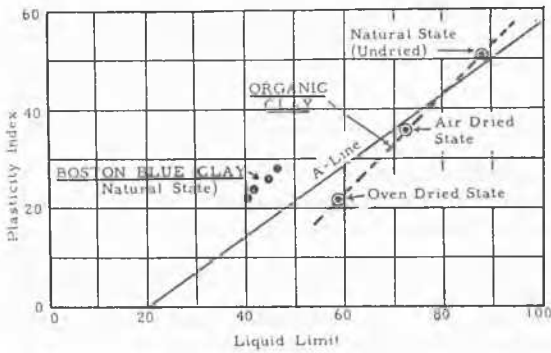


Fig. 2 Plasticity Chart Showing Results of Liquid and Plastic Limit Tests  
Diagramme donnant les résultats des essais de limite de plasticité et de limite de liquidité

**Boston Blue Clay.**—An inorganic, silty clay of low to medium plasticity (*CL*), firm and brittle in undisturbed state but soft and sticky when remolded.

The samples used in this investigation were taken at a depth of about 25 ft. by means of a 5-inch thin wall tube sampler. Consolidation tests showed that the preconsolidation load was about 4 kg/cm<sup>2</sup>, thus greatly in excess of the existing overburden. The natural water content was about 35%, which is slightly below the liquid limit. The results of liquid and plastic limit tests are shown in Fig. 2.

### Apparatus and Test Procedures

In order to reduce the piston friction of earlier designs of triaxial apparatus, most apparatus at Harvard were rebuilt starting in 1940 to the use of small-diameter pistons. This modification, together with rotation of the piston, reduced piston friction to a tolerable amount. Rotation of the piston necessitated a rather complicated design of the caps, and unless the piston were rotated continuously, appreciable friction would still develop in long-time tests. For these reasons efforts were directed toward the development of a piston supported by ball bushings which finally led to the design in 1949 of improved triaxial compression apparatus illustrated in Fig. 3.

The unique design of the ball bushing permits unlimited axial movement with a minimum of friction, but not rotation (in contrast to ball bearings). In order to adapt the ball bushing to triaxial apparatus, it was necessary to locate a small steel sleeve midway between the two ball bushings, to prevent excessive leakage.

In order to demonstrate the advantage of the ball bushings in reducing friction due to eccentricity, tests were performed by applying a horizontal force against the piston in various types of apparatus, one inch below the bottom of the bushing, and measuring the axial load required to move the piston. The results of these tests are illustrated in Fig. 4, which shows the great superiority of pistons guided by ball bushings.

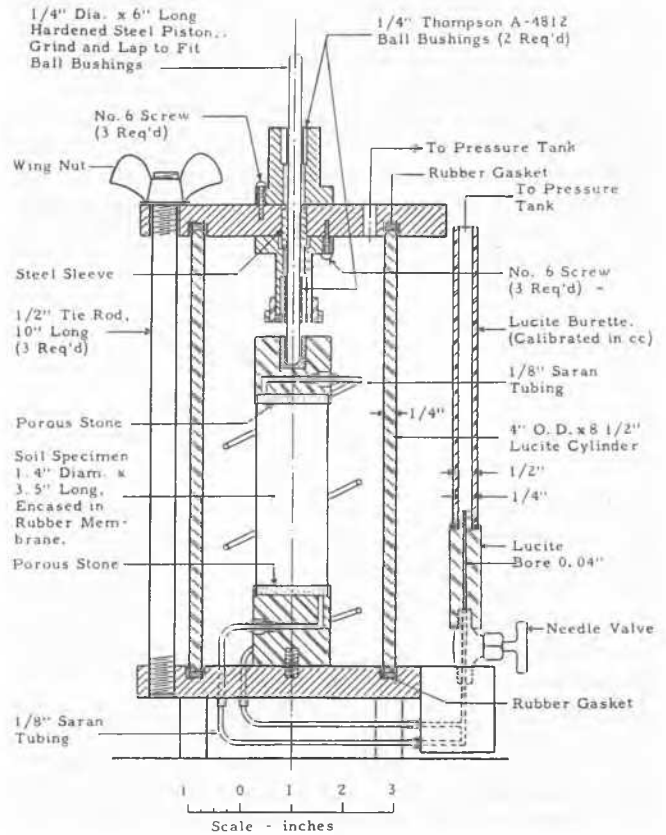


Fig. 3 Sketch of Harvard Triaxial Apparatus with Ball Bushings  
Schéma de l'appareil triaxial de Harvard avec «glissière à billes»

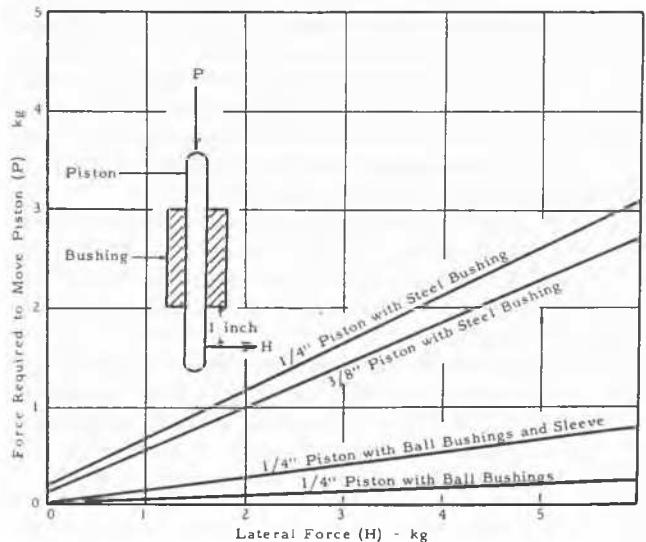


Fig. 4 Effect of Lateral Force on Piston Friction in Triaxial Apparatus  
Influence d'une force latérale sur le frottement du piston dans l'appareil triaxial

Additional tests were made to determine if the axial force required to start the piston in motion might build up during periods when the piston was at rest. In these tests the horizontal force against the piston was applied by a calibrated spring placed between the wall of the triaxial chamber and the piston. The chamber was filled with castor oil, under pressure, and the axial force required to move the piston was determined. The entire assembly was then left untouched for periods of time up to one week, following which the friction tests were repeated. The results checked those previously reported, and showed conclusively that piston friction does not build up in the ball-bushing type of apparatus during periods of rest.

The air line from the top of the burette (Fig. 3) leads to a system of control valves and pressure gages to permit close adjustment of pore water pressure. Water was used for the chamber fluid in all tests, and to prevent air leakage through the membrane the entire chamber plus about 10 ft. of  $\frac{1}{8}$ -inch O. D. Saran tubing was filled with water.

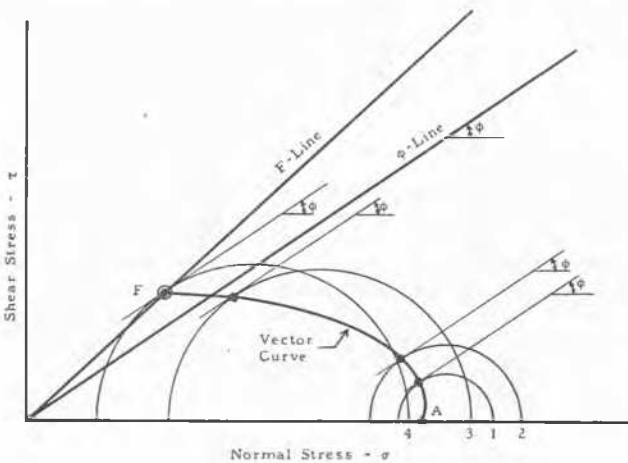


Fig. 5 Procedure Used to Plot Vector Curve  
Procédé utilisé pour construire la courbe des vecteurs

When pore pressure measurements were made, the Qc tests were performed in the following manner:—

(1) With the apparatus completely assembled and with that drainage valve closed which connects the burette with the inside of the specimen, the burette was placed under an initial pressure ( $u_0$ ) of approximately  $0.5 \text{ kg/cm}^2$ . This initial neutral stress,  $u_0$ , was selected to correspond approximately to the neutral stress *in situ*, to assist in maintaining full saturation.

(2) The chamber pressure was then applied such that it equalled the desired value of  $\sigma_3$  plus  $u_0$ .

(3) The burette valve was opened and dial and burette readings were made at suitable intervals. The time for theoretical 100% consolidation was found to be about 5 hours, but a minimum of 24 hours of full drainage was allowed to minimize secondary time effects.

(4) The water level in the burette was lowered to the capillary section, and increments of axial load were applied at approximately 3 to 5 minutes intervals. The pore-pressure valves were continuously adjusted such that the level of the meniscus in the capillary section neither rose nor fell.

### Vector Curves

In the analysis of test data, curves are used which connect computed points representing the effective normal and shear

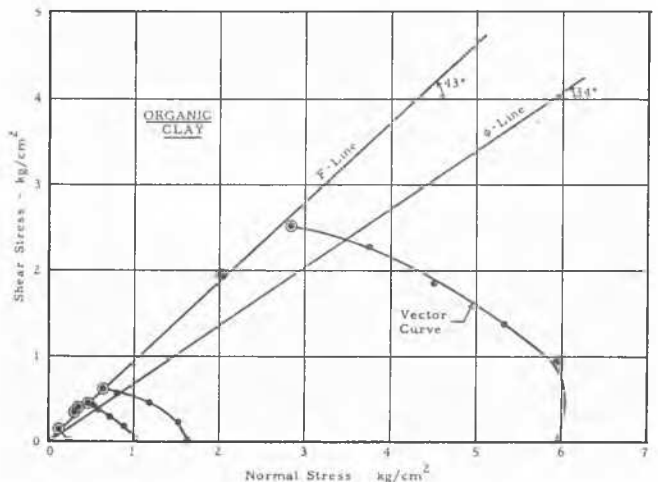


Fig. 6 Results of Triaxial Compression Tests on Organic Clay  
Résultats des essais de compression triaxiale sur une argile organique

stresses on the  $\left(45 + \frac{\phi}{2}\right)$  plane, where  $\phi$  is the angle of internal friction as determined by the slope of the Mohr failure envelope for  $S$  tests above the natural preconsolidation stress. Such curves represent the vector of the resultant effective stress on the  $\left(45 + \frac{\phi}{2}\right)$  plane, and therefore for brevity will be referred to as "vector curves". Fig. 5 illustrates how a vector curve is plotted. Mohr stress circles for effective stresses are derived from neutral stress measurements made during axial loading. Then tangents to the stress circles are drawn with the slope  $\phi$ . The curve connecting the points of tangency is the vector curve. The starting point  $A$  of the vector curve is determined by  $\sigma_3 = \bar{\sigma}_3$  at the start of axial loading. Point  $F$  represents the stress condition at failure and is referred to as the "F-point".

Point 2 (Fig. 5) represents the maximum  $\bar{\sigma}_1$  stress reached in the test, and point 4 the minimum  $\bar{\sigma}_1$  stress. Thus all planes in the specimen are prestressed if one compares the normal stress on any plane at the end of the test with the maximum stress developed on that plane.

### Test Results

The effective stresses from a series of Qc tests on the organic clay are plotted in Fig. 6. The  $F$ -points, shown as double

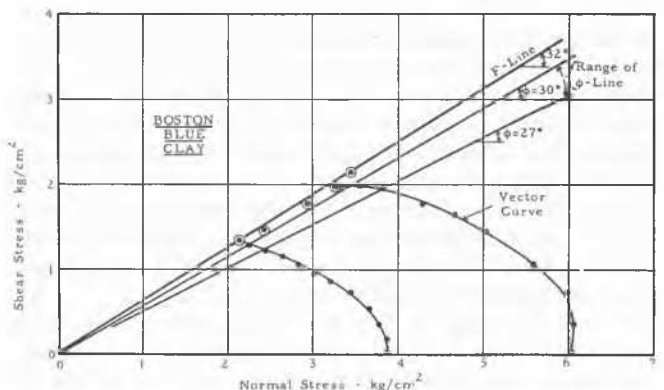


Fig. 7 Results of Triaxial Compression Tests on Boston Blue Clay  
Résultats des essais de compression triaxiale sur une argile bleue de Boston

circles, define approximately a straight line through the origin, and with a slope of  $43^\circ$ . The  $\varphi$ -Line, as determined by two  $S$  tests, was found to be inclined at  $34^\circ$ .

Fig. 7 is a similar plot derived from a series of  $Q_c$  tests on Boston Blue Clay for which the  $F$ -line was found to slope  $32^\circ$ . The angle of internal friction  $\varphi$  from  $S$  tests was found to range between  $27^\circ$  and  $30^\circ$ .

The vector curves shown in Figs. 6 and 7 are typical of those obtained with incremental loading and chamber pressures above the natural preconsolidation pressure. Changes in test procedure cause radical changes in the shape and position of the vector curve, but the end points  $F$  of the vector curves were found to fall always on the same line.

### Relationship Between Effective and Total Stresses for $Q_c$ Tests

Fig. 8 shows the relationship between effective and total stresses for a specimen which is assumed first to be consolidated under an all-around pressure  $\bar{\sigma}_3$  well above the natural pre-stress, and then subjected to axial load increase to failure. The stress circle for total stresses is  $C_1$ , for the effective stresses  $\bar{C}_1$ , and  $A-F$  is the vector curve.

It can be seen from circle  $\bar{C}_1$  that, for the failure condition, the stresses on any plane are less than at the start of the test as shown by point  $A$ . Since past investigations have proved that the strength envelope for  $S$  tests below the preconsolidation load (i.e., for prestressed specimens) curves above the  $\varphi$  line (Fig. 1), one must expect point  $F$  to be located above the  $\varphi$  line. In this connection it is pertinent to recall that past triaxial investigations have shown that in the range of pre-consolidation the deviation of the  $S$  envelope from the  $\varphi$ -Line is also dependent on the length of time allowed for the  $S$  tests. With increasing length of time for the tests the  $S$  envelope comes closer to the  $\varphi$ -Line.

As drawn in Fig. 8, a portion of stress circle  $\bar{C}_1$  lies outside the line connecting point  $F$  with the origin. Although this is

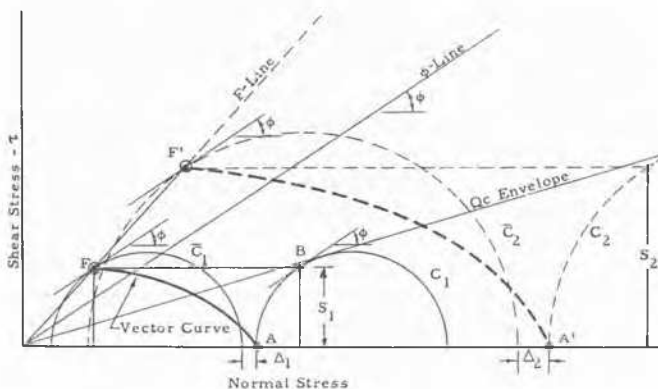


Fig. 8 Relationship between Effective and Total Stresses  
Relation entre les tensions effectives et les tensions totales

not possible for an isotropic material, it is a correct relationship for an anisotropic material. As shown in *Casagrande, Carillo, 1944*, even a small degree of anisotropy can readily explain the relationship between stress circle and  $F$ -line. There appears little doubt that even if a soil is isotropic to start with (which is hardly ever the case), some anisotropy is induced during the axial compression.

The second set of circles in Fig. 8,  $\bar{C}_2$  and  $C_2$ , are shown

principally to assist in visualizing how the  $Q_c$  envelope and the  $F$ -line are derived from a series of tests.

It follows from the above consideration that *all constant volume tests, including the  $Q_c$  tests, are testing the strength of prestressed material*. Therefore, when comparing from such tests the stress circles for total and for effective stresses, one

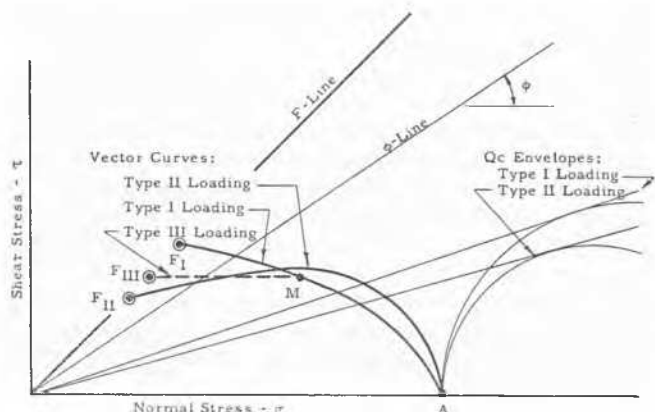


Fig. 9 Effect of Rate of Loading on Vector Curve  
Influence du taux de charge sur la courbe des vecteurs

must not use the  $\varphi$ -Line, but rather the  $F$ -Line. The  $F$ -Line is drawn as a straight line through the origin because the available results in Fig. 6 and 7 indicate this to be its probable shape.

By plotting the effective stress circles through the  $F$  points, instead of tangent to the  $S$  envelope, one obtains a greater separation of the circles for effective and total stresses, thus developing a positive  $\Delta$  value as shown in Fig. 8. Such a separation of the circles was always considered probable for clays having a sensitive structure. By the older procedure of analysis these stress circles would often intersect, even for sensitive clays, which is considered not reasonable because there is no question that for such clays deformation during the test must invite additional consolidation due to partial breakdown of the structure.

### Influence of Rate of Loading on Shape of Vector Curves

In constant volume tests on clays, the shape of the vector curve is influenced by the rate of loading. In Fig. 9 is illustrated the effects of three different types of loading. Type I loading is the type of incremental loading used in this investigation. Type II is loading effected by means of a constant rate of strain and with a total time to failure which is longer than that used for Type I loading. Type III loading proceeds as Type I loading to point  $M$  where the axial load is held constant. If the axial load at point  $M$  exceeds a certain critical value, failure will occur eventually at that load. This type of loading corresponds to the creep-strength tests described in the reference (*Casagrande, Wilson, 1951*). As drawn in Fig. 9, Types II and III loading would represent approximately the same total time of loading.

Depending on the type of loading the vector curve may or may not develop a maximum shear stress  $\tau$  on the critical plane before failure occurs. In particular it was found for Boston Blue clay that such a maximum is developed in constant volume tests in which the loading is effected by applying a constant rate of strain as shown by Type II loading in Fig. 9. By

decreasing the rate of strain in the latter stages of the test one can accentuate the development of a peak in the vector curve, whereas on the other hand a gradual increase in the rate of strain will change the shape of the vector curve such as to form a horizontal approach to the point of failure, or even a steady rise similar to that shown for Type I loading in Fig. 9. In other words, the rate of loading controls the shape of the vector curve, irrespective of whether load increase is effected by stress-control or strain-control.

The shape of the vector curve is also influenced by migration of water within the sample which is due to the fact that even in a triaxial specimen the stress conditions are not homogeneous, but develop non-uniform conditions progressively with increasing strains. Thus, a constant volume test is not a constant void ratio test unless the test is run so fast that no appreciable migration of water can occur. In a standard test on typical clay which is completed generally in about five minutes, this requirement is closely approached. However, if one desires to measure pore pressures, then more time must be allowed for the test and complications develop because of the migration of water.

### Closing Remarks

The material presented in this paper is based on data from a comprehensive research project which is conducted at Har-

vard University for the Corps of Engineers. At this stage of the investigation the practical significance of the  $F$ -Line is not yet sufficiently explored. Perhaps one need not be concerned about the  $F$ -Line, if one uses in the analysis of a problem total stresses and the corresponding apparent angle of internal friction as derived from consolidated-quick tests.

If one desires to analyze strength problems on the basis of effective stresses, one is probably on the safe side if the analysis is based on the angle of internal friction  $\phi$  derived from a series of  $S$  tests. However, when dealing with prestressed clays, the use of the  $S$  envelope in the range of prestress is usually not on the safe side because of long-time swelling effects which are rarely investigated in laboratory tests. Whereas along the branch of the  $S$  envelope above the prestress the effect of the secondary consolidation is to increase the shear strength and thus assure that the results of ordinary  $S$  tests are on the safe side, the strength derived from  $S$  tests in the range of prestress must be generally considered to be on the unsafe side.

### References

- Casagrande, A. and Carrillo, N. (1944):* Shear Failure of Anisotropic Materials. *Journal of the Boston Society of Civil Engineers*, April, Vol. XXXI, No. 2, pp. 74-87.
- Casagrande, A. and Wilson, S. D. (1951):* Effect of Rate of Loading on the Strength of Clays and Shales at Constant Water Content. *Géotechnique*, June, Vol. II, No. 3, pp. 251-263.